RF Coils Characterization in Soil for Wireless Soil Sensing Applications

Weijie Luo[1*], Ramesh Goel[2], Shad Roundy[3], Cody Zesiger[4] and Darrin J. Young[1]
[1]Department of Electrical and Computer Engineering, University of Utah, Salt Lake City, Utah, USA
[2]Department of Civil and Environmental Engineering, University of Utah, Salt Lake City, Utah, USA
[3]Department of Mechanical Engineering, University of Utah, Salt Lake City, Utah, USA
[4]Utah State University, Ogden, Utah, USA
[*]Email: weijie.luo@utah.edu

***Abstract*— This paper presents the characterization results of RF coils in loamy soil with a goal to develop low-cost, long-life, wireless, *in-situ* sensing technologies for monitoring soil health to ensure future sustainable agriculture. Two types of RF coil exhibiting 6 cm-Φ / 9-turn and 12 cm-Φ / 9-turn are employed for the study. The characterization results reveal that coils maximum quality factor takes place around 1 MHz limited by the loamy soil loss. A small gap on the order of 1-2 cm between a coil and surrounding soil can help improve the quality factor significantly. Wireless power transfer efficiency estimation reveals that a sufficient amount of power can be transferred across a soil depth of 30 cm to energize an underground wireless soil sensing network. Further optimized designs are expected to achieve an enhanced performance and extended power transfer distance underground.**

Keywords*— Power transfer through soil, coils characterization in soil, soil loss, wireless soil sensing, wireless power transfer, inductively-coupled power transfer.

I. Introduction

With the world's population expected to surpass 9 billion by 2050, increasing food production threatens soil security, presenting one of the grand challenges of the 21st century [1]. Sustaining high levels of food production depends on healthy soil. Therefore, there is a strong need to develop low-cost, long-life, wireless, *in-situ* sensing technologies for monitoring soil health to ensure future sustainable agriculture. In this work, we propose to develop a wireless underground *in-situ* soil sensing network, depicted in Figure 1, where autonomous vehicles, both ground and aerial, can potentially power or recharge an underground sensor module in a wireless manner as well as communicate with the sensor module for data telemetry [2, 3]. Sensor data may include soil moisture, salinity, temperature, pH, etc., which are indicative of soil health condition. Autonomous vehicles can transfer radio-frequency (RF) power to the sensor module from a power source incorporated inside the vehicles in a close proximity to the ground surface as shown in Figures 1(a) and 1(b). To access farmland covered by tall crops, an unmanned aerial vehicle (UAV) can communicate with an above-ground telemetry post, which is further connected to an underground sensor module as illustrated Figure 1(c).

Inductively-coupled RF power transfer techniques have been widely employed for biomedical, industrial and consumer electronics applications [4-16]. Each application exhibits inherent trade-offs in terms of size of coils, coupling distance, number of coils, operating frequency, intrinsic loss, surrounding medium loss, efficiency, loading, frequency splitting, susceptibility to detuning, etc. We choose inductively-coupled means to investigate its potential to wirelessly transfer power through soil to enable the proposed wireless soil sensing capability.

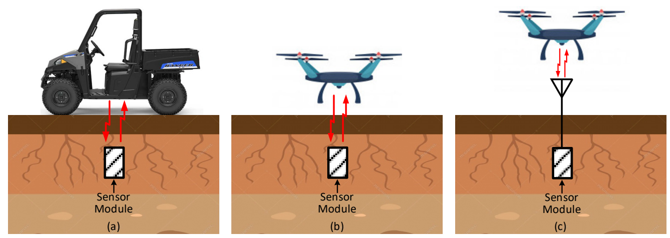

Fig. 1. Wireless underground *in-situ* soil sensing network architecture.

II. Inductively-Coupled Power Transfer Through Soil

Figure 2 presents an inductively-coupled RF power transfer system design diagram, where an RF power is coupled to a secondary coil, L_2, from a primary coil, L_1, tuned to the same frequency through the mutual inductance. The received RF power, which exhibits an AC voltage swing at V_{out} across a load resistor, R_{load}. The AC voltage swing can be further rectified and filtered to produce a nearly constant DC voltage to energize the soil sensing system. It should be noted that the secondary coil represents the coil buried under the ground, whereas the primary coil is above the ground.

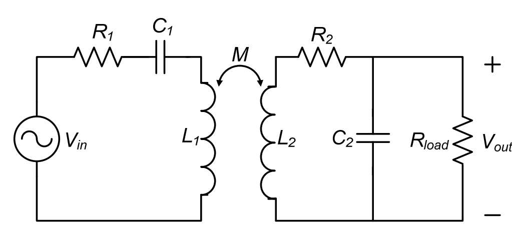

Fig. 2. Inductively-coupled RF power transfer system.

It can be shown that the voltage gain, A_v, from V_{in} to V_{out} can be expressed as [17]:

$$A_v = \frac{V_{out}}{V_{in}} = \frac{\omega^2 L_2 M}{(\omega M)^2 + R_1 R_2 + \frac{R_1 (\omega L_2)^2}{R_{load}}}, \quad (1)$$

where M is the mutual inductance between L_1 and L_2, ω is the tuned resonant frequency of two coils, R_1 and R_2 are the series resistances associated with L_1 and L_2, respectively, representing the loss. Further simplifying the equation results in the following expression:

$$A_v \approx kQ_1Q_2\sqrt{L_2/L_1}\,\frac{1}{1+\beta}, \qquad (2)$$

where k is the coupling factor between L_1 and L_2, Q_1 and Q_2 are the loaded quality factor of the primary coil and unloaded quality factor of the secondary coil, respectively, and β is the ratio between an equivalent serial load resistance of $\frac{(\omega L_2)^2}{R_{load}}$ associated with the secondary coil and the coil's serial resistance of R_2, which can be expressed as $\beta = \frac{(\omega L_2)^2}{R_{load}R_2}$. The power coupling efficiency, $\eta_{coupling}$, defined as the ratio of the power delivered into R_{load} and the power dissipated in the external tuned coil loop, under a weak coupling condition can be further derived as

$$\eta_{coupling} = \frac{k^2Q_1Q_2\beta}{(1+\beta)^2}. \qquad (3)$$

Additional analysis reveals that an optimal condition as a trade-off between the voltage gain and efficiency occurs around β = 1, which represents a power impedance matching between R_{load} and an equivalent parallel resistance from R_2 at the tuned resonant frequency. While the coupling factor, k, remains unchanged with given coils geometry, separation distance and tilting angle, the power transfer efficiency improves with the coils quality factor of Q_1 and Q_2. It is, therefore, highly important to characterize the coils quality factor with the presence of soil to ensure an efficient system design with predictable performance.

III. RF Coils Characterization in Soil

Prototype coils with a diameter of 6 cm and 12 cm are chosen to investigate their feasibility for wireless power transfer through a soil depth between 20 cm to 30 cm, which represents a typical cultivation layer thickness. Further power transfer to a deeper location, for example with a depth of 1 meter, may be required for certain demanding applications. Coils with too few turns will result in low inductance value and low quality factor, while an excessive number of turns will cause a reduced self-resonant frequency, thus limiting the frequency range for wireless power transfer. As a result, a 9-turn coil design is employed for the current study achieving high Q and sufficiently high self-resonance. The prototype coils are implemented by using solid copper wire with a diameter of 0.8 mm and a stranded litz wire with an outer diameter of 0.8 mm. It should be noted that the litz wire is made of 330 strands of 40 µm-Φ copper wires, which is expected to achieve an improved conductivity due to an

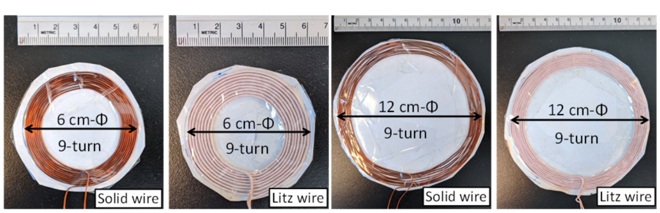

Fig. 3. Photos of RF coils.

enhanced surface area. The prototype coils are presented in Figure 3, showing two coil configurations, namely, 6 cm-Φ / 9-turn and 12 cm-Φ / 9-turn, each made of solid wire and litz wire, respectively. The characterization of each coil is conducted in air, on top of 10 cm thick loamy soil and further buried under a 20 cm thick loamy soil in a laboratory setting by using a network analyzer. A sample of Parleys loam was collected in northern Utah for the coils characterization. Other types of soil such as sandy and clay soil will be considered for coils characterization planned as next step.

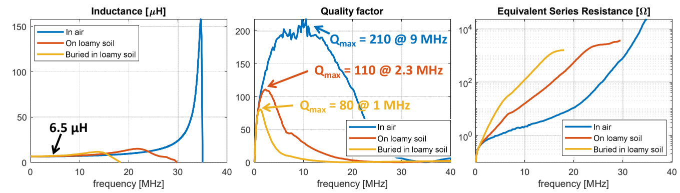

(a) 6 cm-Φ solid wire coil

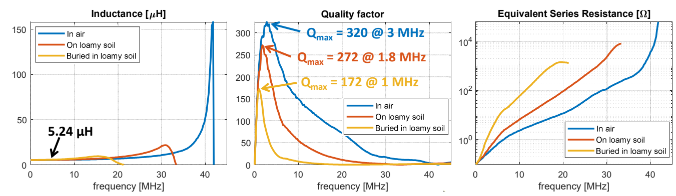

(b) 6 cm-Φ litz wire coil

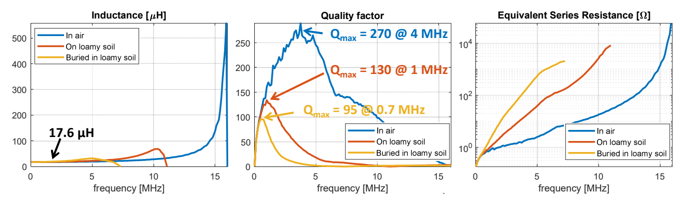

(c) 12 cm-Φ solid wire coil

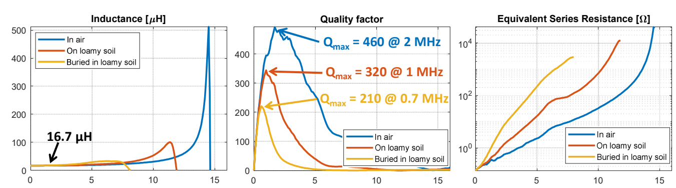

(d) 12 cm-Φ litz wire coil

Fig. 4. Measured inductance, Q and ESR vs. frequency of coils when placed in air, on loamy soil and buried in loamy soil.

Figure 4 shows the measured inductance, Q, and equivalent series resistance (ESR) of the four prototype coils when placed in air, on top of 10 cm thick loamy soil and buried under 20 cm thick loamy soil. The measured ESR includes an inherent loss of the coil as well as loss associated with the soil if any. As shown in Figure 4(a), the 6 cm-Φ solid wire coil has an inductance value of 6.5 µH. The Q_{max} in air is 210 at 9 MHz, which reduces to 110 at 2.3 MHz on the soil and further reduces to 80 at 1 MHz when buried in the soil. Figure 4(b) shows the characterization results of the 6 cm-Φ litz wire coil, which shows an inductance value of 5.24 µH. The Q_{max} in air is 320 at 3 MHz, which reduces to 270 at 1.8 MHz on the soil and further reduces to 172 at 1 MHz when buried in the soil, all of which are higher than Q_{max} of the 6 cm-Φ solid wire coil. The 12 cm-Φ solid wire coil exhibits an inductance value of 17.6 µH as shown in Figure 4(c). Its Q_{max} in air is 270 at 4 MHz. The Q_{max} measured on the soil is 130 at 1 MHz and becomes 95 at 0.7 MHz when buried in the soil. As shown in Figure 4(d), the 12 cm-Φ litz wire coil exhibits an inductance value of 16.7 µH. It also achieves a higher Q_{max} of 460 at 2 MHz, 320 at 1 MHz, and 210 at 0.7 MHz when measured in air, on the soil, and buried in the soil, respectively, compared to the 12 cm-Φ solid wire coil. When the coils are placed on or buried in the soil, the reduction in Q is caused by the soil loss, which increases with frequency. As illustrated in the ESR plots of all the four investigated cases, the ESR of coils buried in the soil increases much faster than the ESR of coils in air above 1 MHz, thus indicating that the loss associated with the loamy soil medium dominants above 1 MHz. For both 6 cm-Φ coils and 12 cm-Φ coils, coils made of litz wire achieve higher Q_{max} under all three conditions, thanks to the inherent low loss of the litz wire.

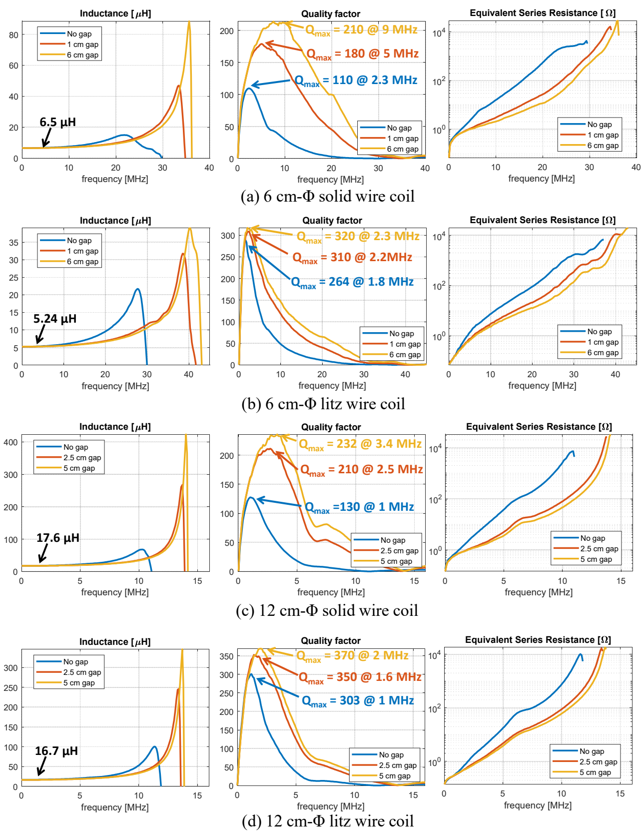

Fig. 5. Measured Q and ESR vs. frequency of coils when positioned above loamy soil with gap.

To further enhance quality factor, coils are positioned above the loamy soil with certain gaps to reduce the loss associated with the soil. As shown in Figure 5(a), Q_{max} of the 6 cm-Φ solid wire coil increases from 110 at 2.3 MHz to 180 at 5 MHz with 1 cm gap, and further increases to 210 at 9 MHz with 6 cm gap. As revealed by the measurement data, a small gap size of 1 cm can introduce a significant Q_{max} improvement of 64%. However, an additional 5 cm gap only yields 17% improvement in Q_{max}. For the 6 cm-Φ litz wire coil as plotted in Figure 5(b), the Q_{max} increases from 264 at 1.8 MHz to 310 at 2.2 MHz and to 324 at 2.3 MHz with 1 cm gap and 6 cm gap, respectively. As can be seen from the plot, the 1 cm gap introduces a 17% increment in Q_{max} while an additional 5 cm gap yields 5% increment in Q_{max}. As shown in Figure 5(c), Q_{max} of the 12 cm-Φ solid wire coil increases from 130 at 1 MHz to 210 at 2.5 MHz and further increases to 232 at 3.5 MHz with 2.5 cm and 5 cm gaps, respectively. A gap of 2.5 cm introduces a significant Q_{max} enhancement of 62%. Further extending the gap to 5 cm only yields 10% increment in Q_{max}. For the 12 cm-Φ litz wire coil as plotted in Figure 5(d), the Q_{max} increases from 303 at 1 MHz to 350 at 1.6 MHz and to 370 at 2.2 MHz with 2.5 cm gap and 5 cm gap, respectively. In other words, a 2.5 cm gap size can introduce 16% improvement in Q_{max}, while further increasing the gap to 5 cm only yields 6% increment. Based on the measurement results, it is evident that a small gap size on the order of 1-2cm between a coil and loamy soil can significantly improve the coils quality factor, and further extending the gap reveals a diminishable improvement. This finding can serve as an important guideline for the coils and overall system package design to ensure a high performance.

Coupling factors between a pair of coils have also been characterized over a distance of 10 cm, 20 cm, and 30 cm. The measured results are presented in Table I.

TABLE I. MEASURED COUPLING FACTOR (K)

Distance	**Coil pairs**		
	6 cm-Φ coil & 6 cm-Φ coil	***6 cm-Φ coil & 12 cm-Φ coil***	***12 cm-Φ coil & 12 cm-Φ coil***
10 cm	3.6×10^{-3}	5.4×10^{-3}	1.9×10^{-2}
20 cm	4.6×10^{-4}	8.7×10^{-4}	3.6×10^{-3}
30 cm	1.2×10^{-4}	2.6×10^{-4}	1.1×10^{-3}

Based on the characterized coupling factors and quality factors, a power transfer efficiency can be estimated revealing that an efficiency of approximately 13% and 1.6% can be achieved by employing a pair of 12 cm-Φ litz wire coils across a loamy soil depth of 20 cm and 30 cm, respectively, under an optimal load of 15 kΩ. Further analysis shows that an external RF power of approximately 0.5 mW and 4.6 mW are required to develop an AC voltage swing with an RMS amplitude of 1V across 15 kΩ, corresponding to a received RF power level of 66 µW, over the 20 cm and 30 cm depths, respectively. An improved performance can be expected by packaging coils with a gap of 1-2 cm from the soil. The received RF power can be used to generate a 2.5V DC output with a current driving capability of approximately 25 µA, which can serve as a design guideline to implement an underground wireless soil sensing network.

IV. CONCLUSION

RF coils have been characterized in loamy soil. Coils made of litz copper wire can achieve higher Q than coils made of solid copper wire. The maximum quality factor occurs around 1 MHz limited by the loamy soil loss. A small gap on the order of 1-2 cm between a coil and surrounding soil can help improve the quality factor significantly. Wireless power transfer efficiency estimation reveals that an external RF power of approximately 0.5 mW and 4.6 mW are required to develop an AC voltage swing with an RMS amplitude of 1V across a load of 15 kΩ, corresponding to a received RF power level of 66 µW, across a loamy soil depth of 20 cm and 30 cm, respectively, which is sufficient to power an underground wireless soil sensing network.

Acknowledgment

The authors would like to acknowledge the research support from the National Science Foundation for this work.

References

[1] IPBES, 2018. Report of the sixth session of the IPBES Plenary.

[2] P. D Mitcheson, et al, "Power electronics for wireless power delivery in synthetic sensor network," Journal of Physics: Conference Series 1052 (1), 012145.

[3] P. D. Mitcheson, David Boyle, George Kkelis, David Yates, Juan Arteaga Saenz, Samer Aldhaher, Eric Yeatman, "Energy-autonomous sensing systems using drones," IEEE Sensors Conference, 2017, pp. 1-3.

[4] P. Cong, N. Chaimanonart, W. H. Ko, and D. J. Young, "A wireless and batteryless 130 milligram 300 μW 10-bit implantable blood pressure sensing microsystem for real-time genetically engineered mice monitoring," IEEE International Solid-State Circuits Conference (ISSCC), San Francisco, February, 2009, pp. 428-429.

[5] P. Cong, N. Chaimanonart, W. H. Ko, and D. J. Young, "A wireless and batteryless 10-bit implantable blood pressure sensing microsystem with adaptive RF powering for real-time genetically engineered mice monitoring," IEEE Journal of Solid-State Circuits, Vol. 44, No. 12, pp. 3631-3644 (Special Issue), December 2009.

[6] P. Cong, W. H. Ko, and D. J. Young, "Wireless batteryless implantable blood pressure monitoring microsystem for small laboratory animals," IEEE Sensors Journal, Vol. 10, No. 2, pp. 243-254, 2010.

[7] D. C. Galbraith, M. Soma, and R. L. White, "A wideband efficient inductive transdermal power and data link with coupling insensitive gain," IEEE Transactions on Biomedical Engineering, Vol. BME-34, No. 4, pp. 265 – 275, April 1987.

[8] P. R. Troyk and G. A. DeMichele, "Inductively-coupled power and data link for neural prostheses using a class-E oscillator and FSK modulation," IEEE International Conference Engineering in Medicine and Biology Society, Vol. 4, pp. 3376 – 3379, September 2003.

[9] P. Mohseni and K. Najafi, "Wireless multichannel biopotential recording using an integrated FM telemetry circuit," IEEE International Conference Engineering in Medicine and Biology Society, pp. 4083 – 4086, September 2004.

[10] W. Liu and M. S. Humayun, "Retinal prosthesis," Technical Digest, IEEE International Solid-State Circuits Conference, pp. 218 – 225, February 2004.

[11] M. Ghovanloo and K. Najafi, "A wideband frequency-shift keying wireless link for inductively powered biomedical implants," IEEE Transaction on Circuits and Systems I, Vol. 51, Issue 12, pp. 2374 – 2383, December 2004.

[12] M. Sawan, Y. Hu, and J. Coulombe, "Wireless smart implants dedicated to multichannel monitoring and microstimulation," IEEE Circuits and Systems Magazine, pp. 21-39, First Quarter, 2005.

[13] R. R. Harrison, "Designing efficient inductive power links for implantable devices," IEEE International Symposium on Circuits and Systems, 2007, pp. 2080-2083.

[14] B. D. Farnsworth, R. J. Triolo and D. J. Young, "Wireless implantable EMG sensing microsystem," IEEE Sensors Conference, October 2008, pp. 1245-1248.

[15] N. Chaimanonart and D. J. Young, "Remote RF powering for industrial strain sensing microsystem," IEEE Sensors Journal, Volume 6, Issue 2, April, pp. 484 – 489, 2006.

[16] N. Chaimanonart, M. A. Suster, and D. J. Young, "Two-channel passive data telemetry with remote RF powering for high-performance wireless and batteryless strain sensing microsystem applications," IEEE Sensors Journal, Volume 10, Issue 8, pp. 1375-1382, 2010.

[17] D. J. Young, P. Cong, M. A. Suster, M. Damaser, "Implantable wireless battery recharging system for bladder pressure chronic monitoring," Lab on a Chip, DOI: 10.1039/C5LC00821B, 2015, 15, 4338-4347.